

# Intramitochondrial Location and Dynamics of *Crithidia fasciculata* Kinetoplast Minicircle Replication Intermediates

Mark E. Drew and Paul T. Englund

Department of Biological Chemistry, Johns Hopkins Medical School, Baltimore, Maryland 21205

**Abstract.** Kinetoplast DNA, the mitochondrial DNA of *Crithidia fasciculata*, is organized into a network containing 5,000 topologically interlocked minicircles. This network, situated within the mitochondrial matrix, is condensed into a disk-shaped structure located near the basal body of the flagellum. Fluorescence in situ hybridization revealed that before their replication, minicircles are released vectorially from the network face nearest the flagellum. Replication initiates in the zone between the flagellar face of the disk and the mitochondrial membrane (we term this region the kinetoflagellar

zone [KFZ]). The replicating minicircles then move to two antipodal sites that flank the disk-shaped network. In later stages of replication, the number of free minicircles increases, accumulating transiently in the KFZ. The final replication events, including primer removal, repair of many of the gaps, and reattachment of the progeny minicircles to the network periphery, are thought to take place within the antipodal sites.

**Key words:** cell cycle • kinetoplast DNA • DNA replication • fluorescence in situ hybridization • trypanosomatid

## Introduction

Kinetoplast DNA (kDNA)<sup>1</sup> is the mitochondrial DNA of trypanosomes and related parasitic protozoa. Unique in nature, kDNA is organized as a single massive network of topologically interlocked DNA circles. The network is situated in the matrix of the cell's single mitochondrion. There are two kinds of circles that form the network. In the parasite *Crithidia fasciculata*, the subject of this study, there are ~25 maxicircles (38 kb) and ~5,000 minicircles (2.5 kb). The maxicircles contain genes similar to those of conventional mitochondrial DNAs in mammals or yeast, and their transcripts undergo RNA editing (addition or deletion of uridine nucleotides at specific internal sites) to produce a functional mRNA. The minicircles encode guide RNAs that control editing specificity. kDNA replication (for reviews see Shlomai, 1994; Shapiro and Englund, 1995) and editing (for reviews see Kable et al., 1997; Estevez and Simpson, 1999) have been previously described.

Because of its network structure, kDNA has an unusual

mechanism of replication. kDNA synthesis differs from that of conventional mitochondrial DNAs in that it occurs only during a discrete phase of the cell cycle, approximately concurrent with the nuclear S phase (Steinert and Van Assel, 1967; Cosgrove and Skeen, 1970; Simpson and Braly, 1970; Woodward and Gull, 1990). In this paper, we focus exclusively on the replication of minicircles. The first step in replication is the release of individual covalently closed minicircles from the network by a topoisomerase (topo). These free minicircles undergo unidirectional replication via  $\theta$  structure intermediates (Englund, 1979). Both progeny minicircles contain gaps. The progeny molecule containing the leading strand has a single gap, whereas the daughter molecule containing the lagging strand has multiple gaps between Okazaki fragments (Kitchin et al., 1984, 1985; Birkenmeyer and Ray, 1986; Birkenmeyer et al., 1987). The Okazaki fragments are unusually small, with most of them <100 nucleotides in size (Kitchin et al., 1984). After segregation, the gapped progeny are attached to the periphery of the network. Just before attachment, many but not all of the gaps are repaired. Because gaps persist in all newly synthesized minicircles, the replicating network develops two zones. A zone of newly replicated gapped minicircles forms around the network periphery, whereas the central zone contains unreplicated minicircles that are covalently closed. As replication proceeds, the central zone shrinks and the peripheral zone enlarges (Pérez-Morga and Englund, 1993b; Guilbride and Englund, 1998) until all of the minicircles have undergone

Address correspondence to Paul T. Englund, Department of Biological Chemistry, Johns Hopkins Medical School, 725 N. Wolfe St., Baltimore, MD 21205. Tel.: (410) 955-3790. Fax: (410) 955-7810. E-mail: penglund@jhmi.edu

<sup>1</sup>Abbreviations used in this paper: dUTP, 5(6)-carboxamidocaproyl-(5-[3-aminoallyl]-2'-deoxy-uridine-5'-triphosphate); F-dUTP, fluorescein-dUTP; kDNA, kinetoplast DNA; KFZ, kinetoflagellar zone; pol, polymerase; SSE-1, structure-specific endonuclease I; TdT, terminal deoxynucleotidyl transferase; topo, topoisomerase; TR, Texas red; UMSBP, universal minicircle sequence binding protein.

replication. This results in a doubled network of 10,000 minicircles, all of which still contain at least one gap. At this time, the remaining gaps are repaired, and the network undergoes scission, a process probably mediated by a topo (Pérez-Morga and Englund, 1993b). The two progeny networks then segregate into each daughter cell at the time of cell division.

A remarkable feature of the kDNA system is that the network and proteins involved in its replication can be visualized at discrete sites within the mitochondrial matrix by fluorescence microscopy. The network, which in isolated form is a planar elliptically shaped structure  $\sim 10$  by  $15 \mu\text{m}$  in size, is condensed in vivo into a disk  $\sim 1 \mu\text{m}$  in diameter and  $\sim 0.3 \mu\text{m}$  in thickness (Shapiro and Englund, 1995). The disk is always positioned in a part of the mitochondrial matrix near the flagellar basal body, and it is aligned such that its faces are perpendicular to the axis of the flagellum. Flanking the disk are two antipodal sites each known to contain enzymes likely involved in replication (see diagram in Fig. 6 for in vivo organization of kDNA network and assorted enzymes). The enzymes are topo II (Melendy et al., 1988), DNA polymerase (pol)  $\beta$  (Ferguson et al., 1992), and structure-specific endonuclease I (SSE-1) (Engel and Ray, 1999), an enzyme that has ribonuclease H activity. The antipodal sites also contain free minicircle replication intermediates (Ferguson et al., 1992; Johnson and Englund, 1998). DNA primase has a different location, positioned above and below the kDNA disk, forming a sandwich-like structure (Li and Englund, 1997; Johnson and Englund, 1999). Understanding the organization of these enzymes and intermediates within the mitochondrial matrix has clarified our knowledge of the replication process. According to the most recently published model (Li and Englund, 1997), covalently closed minicircles are released from the network by a topo. They then encounter primase (and presumably other proteins) to either form initiation complexes that move to the antipodal sites to begin replication or, alternatively, to initiate the replication process immediately. The location of the major part of the replication process is not known, but the final stages, including primer removal (by SSE-1), repair of some of the gaps (by pol  $\beta$ ), and attachment of gapped minicircles to the network periphery (by topo II), likely occur in the antipodal sites. To ensure that newly synthesized minicircles attach uniformly around the network periphery, there appears to be relative movement of the kDNA disk and the antipodal sites during the network replication process (Pérez-Morga and Englund, 1993a). This relative movement apparently occurs in *C. fasciculata* but not in *Trypanosoma brucei* (Ferguson et al., 1994).

In this study, we have used fluorescence microscopy as well as other techniques to investigate the intramitochondrial location and dynamics of free minicircle replication intermediates. Our most surprising finding was that minicircles are released from the network disk in a vectorial manner, from the side of the disk nearest the flagellum. They enter a region that is reported to contain unilateral filaments that are thought to mediate a cytoskeletal association of the basal body of the flagellum with the kDNA disk (Robinson and Gull, 1991; Gull, 1999; Ploubidou et al., 1999). We term this region, which is the site of initiation of minicircle replication, the kinetoflagellar zone (KFZ). The

minicircle progeny then migrate from this zone to the antipodal sites for the final events in replication.

## Materials and Methods

### Cell Culture and DNA Isolation

*C. fasciculata* was cultured at room temperature in brain heart infusion (Difco Laboratories, Inc.) containing  $10 \mu\text{g/ml}$  hemin. For all in situ hybridization experiments, the cells were harvested during log phase ( $\sim 5 \times 10^7$  cells/ml). DNA was isolated by lysis with sarkosyl-pronase, treated with RNase, phenol/chloroform extracted, and ethanol precipitated (Ausubel, 1988).

### Probes

As shown previously (Ferguson et al., 1992), FISH probes specific for the minicircle L-strand in a nondenaturing hybridization recognize free minicircle replication intermediates with naturally single-stranded regions (Englund et al., 1982). For the experiments presented here, the probes were synthesized by a two-step PCR method using purified *C. fasciculata* kDNA as template. Initially, a 62-bp region (nucleotides 430–491) of the major minicircle sequence class (Sugisaki and Ray, 1987) was amplified under standard PCR conditions and gel purified (the primers were A, 5'-AGGAAATCCCGTTCAAAAATCG, and B, 5'-CCCGAAATCCAGTTTGCC). To generate a fluorescently labeled strand-specific probe that recognizes the minicircle L-strand (H-1, used in all FISH images shown in this paper),  $\sim 20$  ng of the PCR product from above was used as template in a single primer synthesis reaction ( $100 \mu\text{l}$ ) under the following conditions:  $100 \text{ ng}$  primer A;  $10 \text{ mM}$  each of dATP, dCTP, and dGTP;  $1 \text{ mM}$  fluorescein-12-5(6)-carboxamidocaproyl-(5-[3-aminoallyl]-2'-deoxy-uridine-5'-triphosphate) (dUTP) (Roche Molecular Biochemicals);  $1.5 \text{ mM}$   $\text{MgCl}_2$ ; and  $10 \text{ U}$  Taq DNA pol. The reaction was performed at  $50^\circ\text{C}$ ,  $30 \text{ s}$  for annealing, followed by denaturation at  $94^\circ\text{C}$ ,  $30 \text{ s}$ , for a total of 60 cycles (no extension hold time was used because of the short length of product formed). The probe was then purified by ethanol precipitation. This method was used to make two other probes recognizing the L-strand (H-2, corresponding to nucleotides 2505–86, and H-3, corresponding to nucleotides 1148–1211), as well as three probes recognizing the H-strand (L-1, corresponding to nucleotides 430–491; L-2, corresponding to nucleotides 2505–86; and L-3, corresponding to nucleotides 1148–1211).

### In Situ Hybridization

In this procedure, the target DNA was not denatured. Therefore, only free minicircle replication intermediates with single-stranded regions were detected by the strand-specific probe (Ferguson et al., 1992). All operations were at room temperature unless otherwise noted. Before fixation, parasites were harvested by centrifugation ( $1,000 \text{ g}$ ,  $5 \text{ min}$ ), washed twice in  $1 \text{ vol.}$  of PBS, and resuspended to  $5 \times 10^7$  cells/ml. Cell suspension ( $50 \mu\text{l}$ ) was applied to each 6-mm well of an eight-well microscope slide (Electron Microscopy Sciences), which had been previously coated with  $0.1\%$  poly-L-lysine solution (Sigma-Aldrich). Slides were placed in a humidified chamber for  $15 \text{ min}$  to allow cells to adhere. The slides were washed in PBS, immersed ( $10 \text{ min}$ ) in a Coplin jar containing  $50 \text{ ml}$  of  $3.5\%$  paraformaldehyde in PBS, and then immersed ( $10 \text{ min}$ ) in  $3.5\%$  paraformaldehyde,  $0.1\%$  Triton X-100. Slides were washed three times ( $5 \text{ min}$ ) in PBS, treated with  $10 \text{ mM}$  Tris-HCl (pH 8.0),  $5 \text{ mM}$  EDTA,  $150 \text{ mM}$  NaCl, and  $0.5\%$  SDS ( $1 \text{ h}$ ,  $37^\circ\text{C}$ ), and washed three more times ( $5 \text{ min}$ ) in PBS.

Before hybridization, slides were incubated in FISH equilibration buffer ( $50\%$  formamide,  $2\times \text{SSC}$ ) for  $30 \text{ min}$ . Equilibration buffer was removed, and the probe was applied at a concentration of  $2.5 \text{ ng}/\mu\text{l}$  in FISH hybridization buffer ( $50\%$  formamide,  $2\times \text{SSC}$ ,  $10\%$  dextran sulfate,  $100 \mu\text{g/ml}$  sheared salmon sperm DNA) in a volume of  $10 \mu\text{l}$  per 6-mm well. A coverslip was placed on the slide, and its edges sealed with rubber cement. Slides were placed in a humid chamber and incubated for  $18 \text{ h}$  at  $37^\circ\text{C}$ . Coverslips were carefully removed, and the slides were washed three times ( $5 \text{ min}$ ,  $37^\circ\text{C}$ ) in  $50\%$  formamide,  $0.1\%$  Tween 20. Slides were then incubated ( $2 \text{ min}$ ,  $37^\circ\text{C}$ ) in  $2\times \text{SSC}$ ,  $0.1\%$  Tween 20, washed twice with PBS ( $5 \text{ min}$ ), and subjected to terminal deoxynucleotidyl transferase (TdT) labeling (below).

## Fluorescent Labeling of Minicircle Gaps with TdT

In situ labeling of the gaps in replicating minicircles after FISH was performed as described (Johnson and Englund, 1998). All operations were at room temperature unless otherwise noted. In brief, slides were incubated for 10 min with 20  $\mu$ l/well of TdT equilibration buffer (200 mM potassium cacodylate, 25 mM Tris-HCl, pH 6.6, 2.25 mM CoCl<sub>2</sub>, 0.25 mg/ml BSA). Equilibration buffer was removed, followed by incubation for 30 min in 10  $\mu$ l of TdT reaction mix containing 200 mM potassium cacodylate, 25 mM Tris-HCl, pH 6.6, 2.25 mM CoCl<sub>2</sub>, 0.25 mg/ml BSA, 10  $\mu$ M dATP, 2.5  $\mu$ M Texas red (TR)-dUTP (Roche), and 4 U TdT (Roche). Slides were then washed three times for 5 min in 4 $\times$  SSC, 0.1% Tween 20 (final wash containing 1.0  $\mu$ g/ml DAPI), followed by 2 washes (5 min, 37°C) in 2 $\times$  SSC, 0.1% Tween 20. Antifade was added (SloFade Light; Molecular Probes), and coverslips were sealed with nail polish. Labeling of gapped minicircles in isolated networks was performed as described (Guilbride and Englund, 1998) using TdT reaction conditions described above with fluorescein-dUTP (F-dUTP).

## Fluorescence Microscopy

Fluorescence microscopy and digital image acquisition were carried out using an Axioskop microscope (Carl Zeiss, Inc.) equipped with a cooled charge-coupled device camera (SenSys; Photometrics Ltd.) operated with IPLab software (Scanalytics, Inc.). All images were acquired using a 100 $\times$ , 1.3 NA Plan-Neofluar oil immersion objective. DAPI, fluorescein, and TR channels were imaged using a multi-channel emission filter set (model 84000; Chroma Technology Corp.) fitted with individual excitation filters housed in a computer-driven filter wheel (Ludl Electronic Products Ltd.). Proper registration was confirmed by examination of 0.5- $\mu$ m beads that fluoresce under the three channels used (TetraSpeck Microspheres; Molecular Probes).

## Fluorescence Quantitation

We developed this computer-based assay to analyze the FISH patterns on hundreds of cells. Automation scripts were written using the IPLab software (Scanalytics, Inc.) for both collection and analysis of fluorescence images. In brief, fields of cells (each containing  $\sim$ 30 cells) were chosen randomly and manually focused by visualization in the DAPI channel. Images of all four channels (DAPI, fluorescein, TR, and phase-contrast) were automatically captured using predetermined exposure times and then saved to the computer's hard drive. This process was repeated until the desired number of fields was obtained (50 fields took  $\sim$ 3.5 h). The automated analysis of the stored images was then performed in the following manner. Each set of three fluorescent images was recalled, and using the DAPI image, the kDNA networks were automatically identified based on pixel intensity and by minimum and maximum size limits. The pixels comprising each network were defined as a segment, and each segment was then expanded radially by two pixels to include all fluorescence associated with the kDNA. The average size of an expanded segment was  $0.53 \pm 0.26 \mu\text{m}^2$  ( $\sim$ 116 pixels). Intensity values were extracted for the expanded segment regions in all three fluorescent images. Each segment (corresponding to a kDNA network) was assigned an identification number, and the image was resaved. Fluorescence intensity data of each segment was transferred to spreadsheet software and stored for analysis.

## Cell Synchronization

Synchronization of cells was essentially as described (Pasion et al., 1994). In brief, cells were grown to midlog phase ( $\sim 3 \times 10^7$  cells/ml), diluted to  $10^7$  cells/ml, and incubated for 6 h in medium containing 200  $\mu$ g/ml hydroxyurea. Cells were then washed and resuspended in fresh medium and sampled at 30-min intervals.

## Results

### Minicircle Replication Intermediates Are Detected in Three Regions Surrounding the kDNA Disk

In a previous study using FISH with a minicircle probe in which we did not denature the target cellular DNA, we found specific fluorescence corresponding to free minicircle replication intermediates in the antipodal sites (Ferguson et al., 1992).

Using fluorescently modified nucleotides to generate small DNA probes, we have now improved this FISH procedure. With the H-1 probe, we confirmed our previous finding that minicircle fluorescence is localized in the antipodal sites, but we also found fluorescence in the KFZ (between the kDNA disk and the mitochondrial membrane nearest the flagellum). There were two distinct patterns of fluorescence. In the first pattern, there was minicircle fluorescence predominantly in the antipodal sites, but there was also a weak FISH signal in the KFZ (Fig. 1 A). In the second pattern of fluorescence, there was a minicircle FISH signal in the antipodal sites, as in the first pattern, but in addition the KFZ had strong fluorescence (Fig. 1 B). In this case, the fluorescence in the KFZ was distinct from that in the two antipodal sites and formed a separate focus. Fig. 1 C confirms this latter pattern. It shows a cell in which the kinetoplast disk had tipped, so that one face is visible ( $\sim$ 10% of cells have the kDNA disk in this orientation). The central zone of FISH, marked by an arrowhead, is clearly visible and is flanked by the two antipodal sites. Fig. 1 D shows an example of a whole cell of the type shown in Fig. 1 B, except that we have also labeled the gaps of newly replicated minicircles with TR-dUTP using TdT. This treatment labels gaps in both free minicircles and network minicircles. However, the free minicircles in the antipodal sites are much more intensely labeled because they are more heavily gapped (Kitchin et al., 1984, 1985; Johnson and Englund, 1998). A color merge of all three fluorescence labels demonstrates that the TR-dUTP signal from the antipodal sites colocalizes with the FISH signal (yielding a yellow color). Also, the color merge confirms the location of free minicircles in the KFZ.

In this experiment, we found no cells with FISH fluorescence exclusively in the KFZ (with none in the antipodal sites). In other experiments (not shown), we found fluorescence patterns exactly like that in Fig. 1, A and B, with two other probes (H-2 and H-3) that recognize the L-strand, but we found no hybridization with probes recognizing the H-strand (L-1, L-2, and L-3). The specificity for L-strand agrees with findings in our previous study (Ferguson et al., 1992).

### The Localization of Replicating Free Minicircles Is Coordinated with the Extent of Network Replication

We found it striking that there are two distinct patterns of free minicircle fluorescence (shown in Fig. 1, A and B), and therefore we next examined whether the expression of these two patterns is coordinated with the cell cycle. To explore this possibility, we developed a fluorescence quantitation procedure in which we could, in as little as 4 h, collect and analyze data from  $\sim$ 1,000 cells on a single microscope slide. We used cells from a log phase asynchronous culture, which were labeled with three different fluorescent dyes (see Table I for description of fluorescent labels). For each cell, we collected images in all three fluorescence channels as well as a phase-contrast image. We developed an automated script using IPLab software to identify automatically the kDNA networks in the DAPI channel based on their size and fluorescence intensity (DAPI-stained nuclei do not meet the criteria because their size is too large and their DAPI staining is too weak).

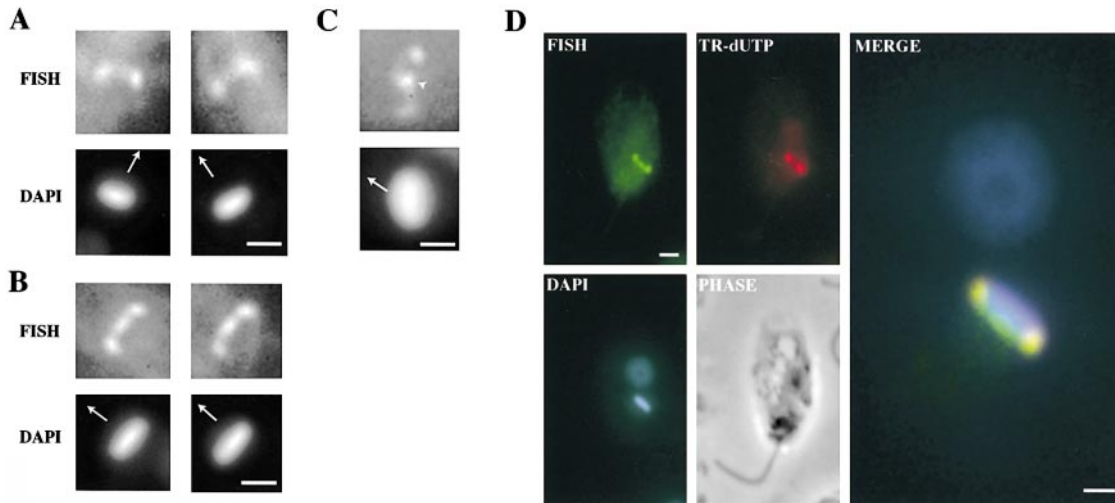


**Figure 1.** Patterns of localization of free minicircle replication intermediates as determined by FISH. The probe (H-1) was fluorescein labeled, and the cellular DNA was not denatured. Images in A–C show FISH labeling, marking location of free minicircles (top), and DAPI labeling, showing the kDNA disk (bottom). In A and B, the disk's edge is visualized in the DAPI images (~90% of cells have this orientation). Arrows point towards the flagellum. (A) There is only weak minicircle fluorescence near the face of the kDNA disk nearest the flagellum. (B) There is strong fluorescence in this region. (C) Shows a cell with a naturally tipped kDNA disk so that one face is visualized (~10% have this orientation). Free minicircles adjacent to the face of the kDNA disk are marked by an arrowhead, and this region is flanked by the antipodal sites. (D) Shows images of a cell labeled with FISH, DAPI (as in A–C), TR-dUTP (to label gaps in network and free minicircles), and a phase-contrast image. Merge is a magnified view of the kDNA from this cell. We did not easily detect the gapped minicircles in the KFZ using TR-dUTP (faint labeling is seen in some cells), however they were clearly detected using the higher quantum efficiency chromophore Alexa-488-dUTP (Molecular Probes) (see Abu-Elneel et al., 2001, page 725, this issue). Bars: (A–D) 1.0  $\mu\text{m}$ ; (D, merge) 0.5  $\mu\text{m}$ .

We then collected the fluorescence intensity values for DAPI, fluorescein, and TR in the region within and surrounding each kDNA network, and transferred these data to spreadsheet software. A powerful feature of this method is that, during the analysis, the software assigned each kDNA network a unique identification number that was permanently recorded on a copy of the image. This allowed us to revisit specific images and visually examine any interesting cell in each of the four recorded channels.

We used this method to analyze ~1,000 cells to determine whether the pattern of free minicircle fluorescence detected by FISH exhibited cell cycle dependence. Fig. 2 A shows the DAPI intensity values (arbitrary units) of 1,036 individual kDNA networks. We then measured the TR fluorescence associated with each network to identify those that were undergoing kDNA replication. There were 254 TR-positive cells, indicating that ~25% were in the process of replicating their kDNA. The DAPI intensity of these replicating kDNA networks is shown in Fig. 2 B, with most of the networks having a value between 1 and 2. In contrast, the 782 cells with nonreplicating kDNA

(TR-negative), which are shown in Fig. 2 C, had an average DAPI fluorescence of only 0.98. Furthermore, plotting of the TR-dUTP intensity for each network against its DAPI intensity (Fig. 2 D) showed a significant correlation ( $r = 0.69$ ). All of these results confirm, as expected, that the DAPI fluorescence intensity gives a rough measure of the extent of kDNA replication. Interestingly, there was only a small population of networks with a 2 $\times$  kDNA content, indicating that the completely replicated unrepaired network is a short-lived species. Next, we visually examined the FISH pattern in each of the 254 cells with replicating kDNA and determined whether they had weak (as in Fig. 1 A) or strong (as in Fig. 1 B) fluorescence in the KFZ. We found that 153 of these replicating networks had an identifiable pattern of free minicircle localization, whereas the remaining 101 were uninterpretable due to improper focal plane or cell orientation. We then plotted the FISH intensity values against the DAPI intensity values for each of these 153 networks. From this graph, shown in Fig. 3, we made two important observations.

**Table I. Fluorescent Labels Used in Experiment in Fig. 2**

Fluorescent label	Target in cell	Purpose
DAPI	Nucleus, kDNA	To identify the kDNA network; fluorescence intensity is proportional to extent of kDNA replication
TdT-incorporated TR-dUTP	Minicircles (free or network bound) that contain gaps* <sup>‡</sup>	To label minicircles that have undergone replication
FISH with fluorescein-labeled minicircle probe	Minicircle replication intermediates with single-stranded regions (Englund et al., 1982)	To identify the location of free minicircle replication intermediates

\*Free minicircles give a much higher signal because they are multiply gapped ( $\leq 40$  gaps per minicircle) (Kitchin et al., 1984). Network-bound gapped minicircles contain much fewer gaps (Kitchin et al., 1985).

<sup>‡</sup>This method could also detect gapped maxicircles but, given that maxicircles constitute only ~7% of the kDNA, it is unlikely that they contribute significantly to the signal.

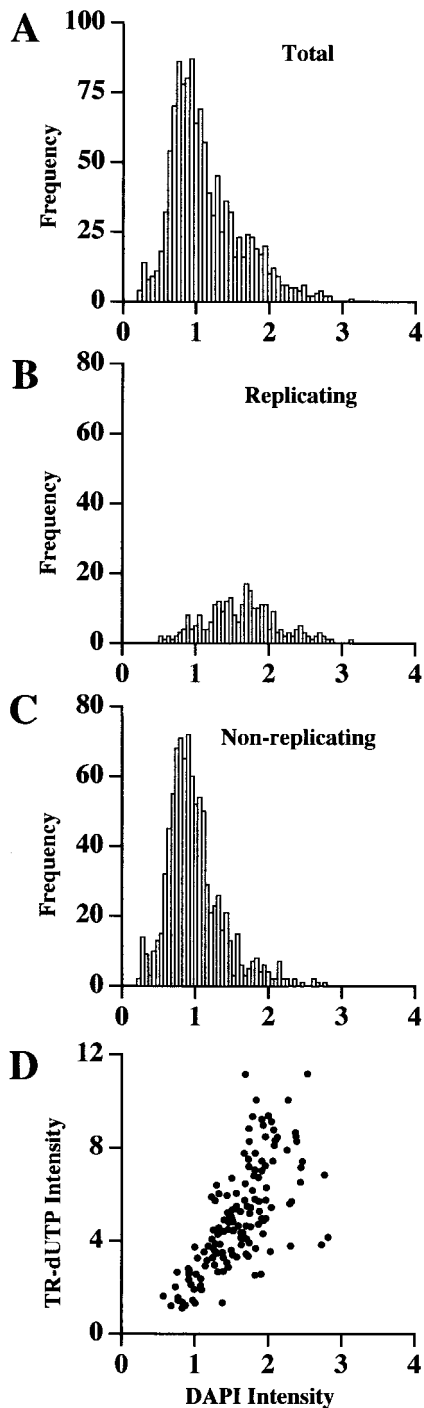


**Figure 2.** DAPI fluorescence analysis of individual kDNA networks in situ. (A) Shows the distribution of DAPI intensity values from 1,036 automatically identified kDNA networks in an asynchronous log-phase cell culture. (B) Shows the distribution of 254 of the networks from A that were identified as replicating based on labeling with TR-dUTP. (C) Shows the distribution of 782 nonreplicating kDNA networks from A that did not label with TR-dUTP. (D) Shows the intensity values of TR-dUTP-labeled networks plotted against their DAPI intensity. DAPI and TR-dUTP intensity values are in arbitrary units.

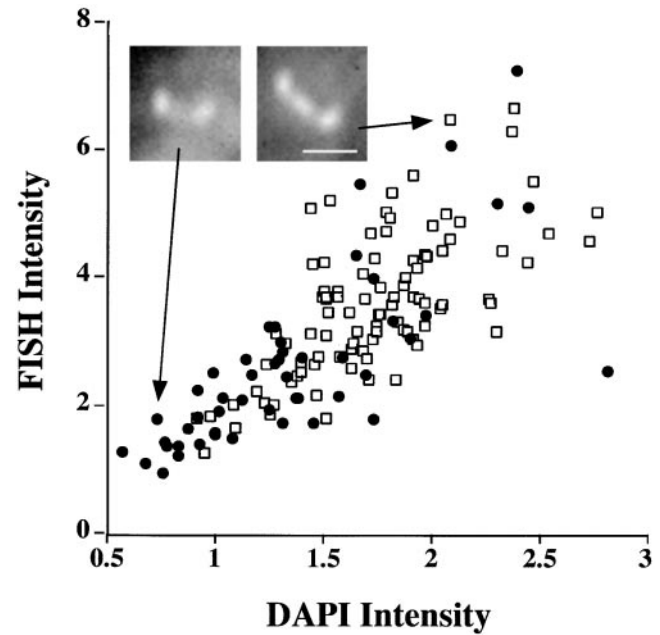


**Figure 3.** Minicircle hybridization (determined by FISH) as a function of DAPI fluorescence. Cells undergoing minicircle replication from Fig. 2 B (detected by TR-dUTP labeling) were each evaluated for intensity of both FISH and DAPI labeling. Of the 254 cells undergoing replication, 153 had an interpretable pattern of FISH. Each of these cells was then individually assessed to determine whether they had weak (●) or strong (□) minicircle fluorescence on the flagellar face of the kDNA disk. Values for fluorescence intensity are arbitrary. Bar, 1.0  $\mu\text{m}$ .

First, we discovered a distinct correlation of the localization pattern of free minicircles (as identified by FISH) with the extent of network replication (as determined by DAPI fluorescence). Cells with weak minicircle fluorescence in the KFZ (Fig. 3, ●) are most abundant in the early stages of replication (51 examples) and have an average DAPI fluorescence intensity of 1.25. In contrast, those with strong minicircle fluorescence in both the antipodal sites and the KFZ (Fig. 3, □) are more abundant at later stages of replication (102 examples), and have an average DAPI fluorescence of 1.83. Consistent with this finding is the fact that the DAPI-stained kDNA disk was usually larger (in diameter) in cells with a strong FISH signal on the flagellar face (Fig. 1, compare A with B).

The second observation was that the FISH intensity values spanned an approximate sixfold range and were roughly proportional to the DAPI intensity values. A likely interpretation of this finding is that, in the early stages of replication, the number of replicating free minicircles is low, and that this value increases as kDNA synthesis progresses. In the following section, we use a completely different experimental approach to test this interpretation.

### **Free Minicircles Rise in Copy Number during kDNA Synthesis**

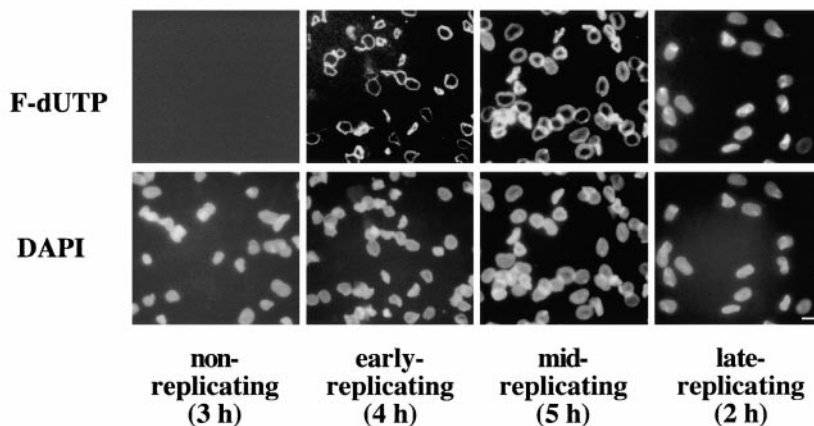
To directly measure the free minicircle copy number at different stages of kDNA replication, we arrested parasites at the G1/S boundary by treatment with hydroxyurea (Pasion et al., 1994). We then washed the parasites free of

hydroxyurea and sampled the culture at 30-min intervals for two cell division cycles. We analyzed parasites from each time point in two ways. First, to assess the synchrony of kDNA synthesis, we purified the kDNA networks from cells at each time point, labeled the replicating networks *in vitro* with TdT, and used fluorescence microscopy to evaluate the distribution of gapped minicircles (Guilbride and Englund, 1998). Fig. 4 A shows representative fields of kDNA networks from cells sampled at various time points during synthesis. Networks in early stages of replication (0.5 and 4 h) have a thin ring of gapped minicircles around the network periphery. Networks at intermediate stages of replication (1.5 and 5 h) have a thicker peripheral ring of gapped minicircles. Networks that contain gapped minicircles throughout (2 and 5.5 h) must be at a late stage of replication. Finally, nonreplicative networks (3 and 6 h) contain no gapped minicircles. The bar graph in Fig. 4 B presents the fraction of each stage of network present at each time point. These results prove that treatment with hydroxyurea results in parasite populations in which the synthesis of kDNA is highly synchronized. See Guilbride

and Englund (1998) for an image of kDNA networks from an asynchronous population.

To quantitate free minicircles, we then purified total cell DNA from a sample at each time point and performed a Southern hybridization using a  $^{32}\text{P}$ -labeled minicircle probe. This method allowed resolution of the major free minicircle species (singly gapped, multiply gapped, and covalently closed; Kitchin et al., 1985) as shown in Fig. 5 A, lane 1. To quantitate the abundance of free minicircle replication intermediates relative to the total minicircle DNA (including that in networks), we digested a sample with XhoI, an enzyme that cleaves virtually all of the minicircles (both free and network bound) at a single site (Fig. 5 A, lane 2). We then measured the amount of each free minicircle species relative to the total amount of minicircle DNA, revealing the fraction of each species at each time point in the cell cycle. Fig. 5 B shows the results of this analysis. At each time point, the underlined number gives the sum of all three minicircle species as a percentage of total minicircle DNA. These values range from  $\sim 14\%$  at the beginning of kDNA synthesis (0 or 3.5 h) to  $\sim 27\%$  at

**A**



**B**

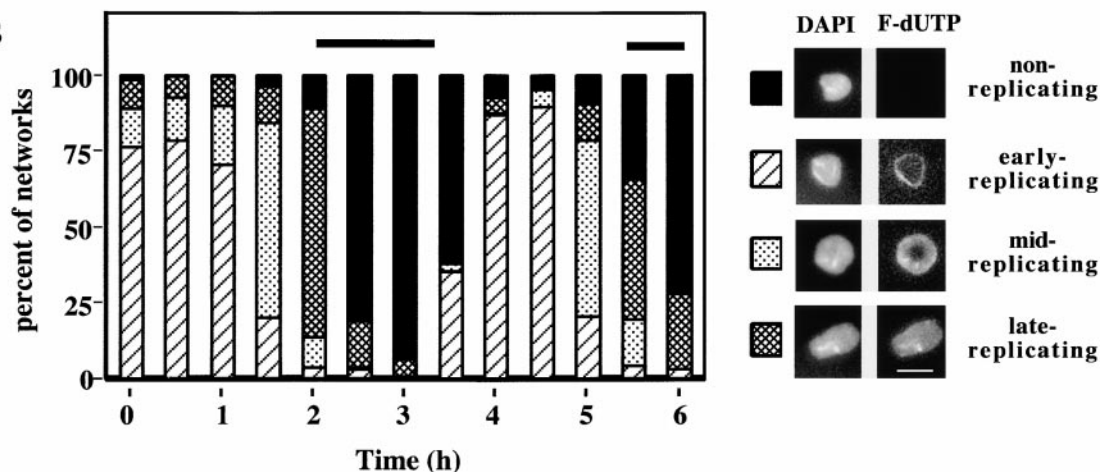


**Figure 4.** Replication status of kDNA networks from a hydroxyurea synchronized cell culture. Networks were isolated, and their gapped minicircles were labeled with F-dUTP using TdT (Guilbride and Englund, 1998). (A) Shows examples, visualized by F-dUTP and DAPI, at nonreplicating (3.0 h), early-replicating (4.0 h), mid-replicating (5.0 h), and late-replicating (2.0 h) stages. (B) Shows the quantitative analysis of kDNA networks from each of the 30-min time points in the cell synchronization experiment ( $>100$  networks counted per time point). Horizontal bars indicate times of peak cell division (compare with Fig. 5). Bars, 10  $\mu\text{m}$ .

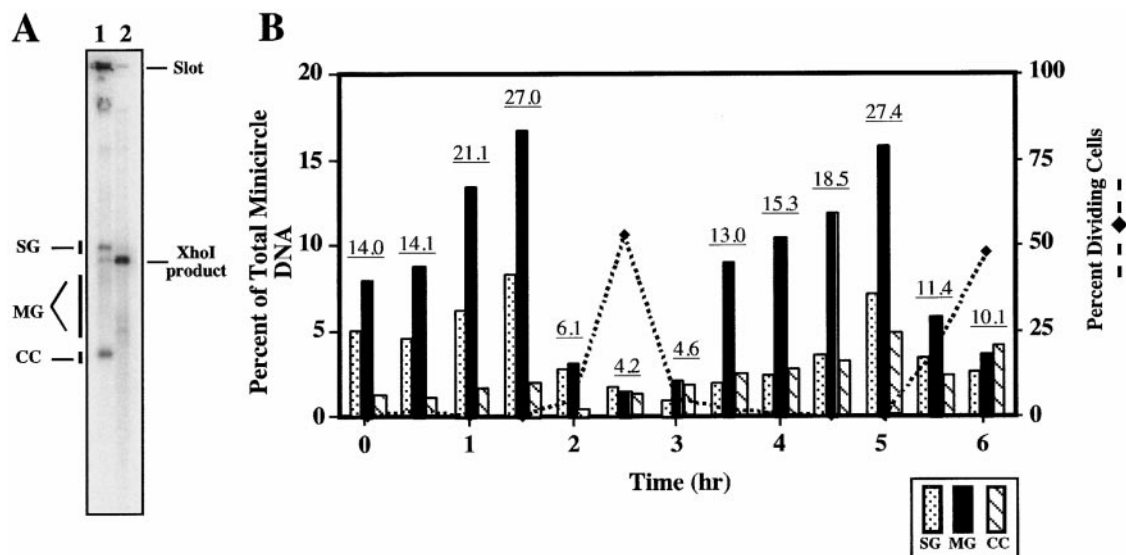


**Figure 5.** Analysis of free minicircle abundance from the synchronized culture used in Fig. 4. Samples were taken at intervals, and total DNA was evaluated by agarose gel electrophoresis (Kitchin et al., 1985). Before transfer to Hybond-N membrane (Amersham Pharmacia Biotech), the gel was treated with 0.2 M HCl for 30 min at room temperature. (A, lane 1) Southern blot (1  $\mu$ g DNA from 0 h time point) hybridized with a  $^{32}$ P-labeled minicircle probe. Radioactivity was measured by phosphorimaging using MacBas software (Fuji Corp.) for singly gapped (SG), multiply gapped (MG), and covalently closed (CC) free minicircles (Kitchin et al., 1984, 1985). (A, lane 2) A sample (0.1  $\mu$ g) from the same time point that was digested with XhoI, an enzyme that makes a single cleavage in virtually all minicircles (Sugisaki and Ray, 1987). Measurement of radioactivity in the XhoI products was used to calculate the percentage of total kDNA in the form of free minicircles. The smear of DNA in the minicircle region in lane 2 is probably due to cross-hybridization of XhoI-digested nuclear DNA (present near the origin in lane 1). (B) Free minicircle population at each time point. Underlined numbers above each time point give percentage of total kDNA in the form of free minicircles. Dotted line shows percentage of cells undergoing division, with peaks at 2.5 and at 6 h.

the end of kDNA synthesis (1.5 or 5.0 h). Therefore, we concluded that the number of free minicircles does in fact increase during network synthesis, as was suggested by the FISH experiments (Fig. 4). We will address in the Discussion the fact that the abundance of multiply gapped free minicircles was two to three times higher than either singly gapped or covalently closed species.

## Discussion

We had found previously, using FISH with a minicircle probe, that replicating minicircles accumulate in the antipodal sites (Ferguson et al., 1992). We have confirmed this finding and, in addition, have shown that free minicircles are also located in the KFZ (Fig. 1). In about one-third of the cells, there is only weak minicircle fluorescence in the KFZ (Fig. 1 A), whereas in the other two-thirds, the fluorescence in this region is quite intense (Fig. 1 B). We never detected free minicircles at the opposite (nuclear) face of the disk, distal to the flagellum.

These results lead us to conclude that minicircles are released vectorially from the kDNA network into the KFZ for the purpose of replication. Further support for vectorial release is provided by the recent discovery that the minicircle origin recognition protein, universal minicircle sequence binding protein (UMSBP), is also located in the KFZ (see Abu-Elneel et al., 2001, page 725, this issue). USBP is likely to be the first protein bound by the free minicircles before their replication, and it presumably assembles other proteins at the origin and triggers initiation

of the replication process (see Tzfati et al., 1995 for properties of USBP). Primase is another key enzyme that should also be involved in the earliest stage of minicircle replication and it too is in the KFZ (Li and Englund, 1997; Johnson and Englund, 1999). However, primase is also located on the opposite face of the kDNA disk, distal to the flagellum. We do not know the function of primase in this second location. However, we can speculate that maxicircle replication occurs at that site and that primase is involved in that process as well. If this speculation is true, it would mean that the replication of minicircles and maxicircles is segregated, with each occurring at a different location in the mitochondrial matrix. Some proteins, like primase, could be involved in both replication mechanisms, whereas others, like USBP, would be specific for minicircles.

An unexpected finding, and the second major conclusion of this paper, is that the copy number of free minicircle replication intermediates increases at later stages of minicircle replication. Evidence for this conclusion comes from measurements of FISH intensity as a function of the extent of kDNA replication (Fig. 3), and also from direct measurements of free minicircle concentration in synchronized cells (Fig. 5 B). In the latter case, we were able to estimate the free minicircle copy number, which ranged from  $\sim$ 14% at the beginning of network replication to  $\sim$ 27% at the later stages. Therefore, the copy number of free minicircles ranges from  $\sim$ 700 to  $\sim$ 2,700. Only  $\sim$ 4% of the minicircles are free during cell division (this small population of free minicircles could actually be from replicating cells, present because of imperfect synchrony in the

cell population). We do not know why free minicircles increase in copy number during the period of kDNA synthesis. One possibility is that a step in either minicircle replication or network attachment is rate limiting, causing a piling up of some free minicircle intermediates. Our measurements (Fig. 5 B) of each type of free minicircle (covalently closed, multiply gapped, and singly gapped) agree with previous measurements indicating that covalently closed minicircles account for ~20% of the total population (Englund, 1979) and multiply gapped minicircles are about threefold more abundant than singly gapped (Kitchin et al., 1985). The reason for the abundance of multiply gapped molecules is that their attachment to the network is delayed (Kitchin et al., 1984).

A third conclusion of this paper is that free minicircles accumulate in the KFZ only in the latter stages of kDNA replication (Fig. 3). This observation depended on our FISH quantitation in which we examined the pattern of free minicircle hybridization as a function of DAPI fluorescence intensity in ~1,000 cells from an asynchronous cell culture (Fig. 3). We do not know why free minicircles

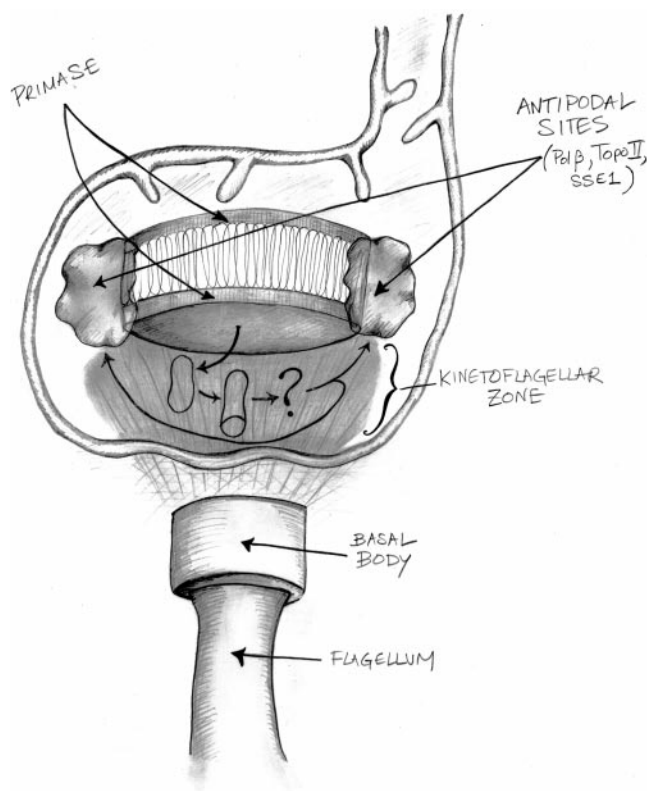


**Figure 6.** Current model of minicircle replication. The kDNA disk is composed of minicircles that are stretched parallel to the axis of the flagellum. Minicircles are released from the central region of the kDNA disk into the KFZ where they encounter proteins such as UMSBP (see Abu-Elneel et al., 2001, page 725, this issue) and primase to begin replication. The minicircles then migrate, through an unknown mechanism, to the antipodal sites where enzymes necessary for their repair (SSE1 and Pol  $\beta$ ) and reattachment (Topo II) are located. The concentration of replicating minicircles in the KFZ increases during kDNA S phase, possibly because of a saturation of the antipodal sites. The extent of minicircle replication within the KFZ is not yet known. Drawing by Kimberly Paul.

accumulate in the KFZ later in the replication process. One possibility is that the antipodal sites become saturated, especially when the free minicircle concentration increases, and this saturation causes a pileup of intermediates in the KFZ.

All of these findings lead to a significant updating of the model for kDNA minicircle replication (Fig. 6). It is now clear that covalently closed minicircles are released vectorially from the network, into the primase-containing KFZ. Given that our FISH probe does not recognize covalently closed minicircles, the replication process must actually initiate in the KFZ. We do not know how far the replication process proceeds in this location, but it is possible that the minicircle is completely replicated (including segregation of the progeny molecules) in the KFZ. Either these progeny minicircles or a partially replicated  $\theta$  structure then moves to the two antipodal sites. If the former is true, it raises the important question of whether minicircles segregate randomly or directionally, an issue that requires further study. Once the minicircles arrive in the antipodal sites the final events in minicircle replication occur. These include the removal of RNA primers (by SSE-1), the repair of many of the gaps (by pol  $\beta$ ), and the attachment to the network of progeny minicircles that still contain at least one gap (by topo II). Finally, after all of the minicircles have been replicated, the remaining gaps are repaired and the network undergoes a topo-mediated remodeling step in which the topology of the network changes (Chen et al., 1995). This is followed by scission of the network, giving rise to the two daughter networks that each contain 5,000 covalently closed minicircles.

We gratefully thank Viiu Klein for providing invaluable technical support and Kimberly Paul for artistic talent. We appreciate comments on the manuscript by Joseph Shlomai, Kawther Abu-Elneel, and members of our laboratory.

This work was supported by grant GM 27608 from the National Institutes of Health.

Submitted: 26 January 2001

Revised: 21 March 2001

Accepted: 21 March 2001

## References

- Ausubel, F.M. 1988. *Current Protocols in Molecular Biology*. Vol. 4. M. Frederick, editor. Wiley-Interscience, New York.
- Abu-Elneel, K., D.R. Robinson, M.E. Drew, P.T. Englund, and J. Shlomai. 2001. Intramitochondrial localization of UMSBP, a trypanosomatid protein that binds kinetoplast minicircle replication origins. *J. Cell Biol.* 153:725–733.
- Birkenmeyer, L., and D.S. Ray. 1986. Replication of kinetoplast DNA in isolated kinetoplasts from *Crithidia fasciculata*. Identification of minicircle DNA replication intermediates. *J. Biol. Chem.* 261:2362–2368.
- Birkenmeyer, L., H. Sugisaki, and D.S. Ray. 1987. Structural characterization of site-specific discontinuities associated with replication origins of minicircle DNA from *Crithidia fasciculata*. *J. Biol. Chem.* 262:2384–2392.
- Chen, J., P.T. Englund, and N.R. Cozzarelli. 1995. Changes in network topology during the replication of kinetoplast DNA. *EMBO (Eur. Mol. Biol. Organ.) J.* 14:6339–6347.
- Cosgrove, W.B., and M.J. Skeen. 1970. The cell cycle in *Crithidia fasciculata*. Temporal relationships between synthesis of deoxyribonucleic acid in the nucleus and in the kinetoplast. *J. Protozool.* 17:172–177.
- Engel, M.L., and D.S. Ray. 1999. The kinetoplast structure-specific endonuclease I is related to the 5' exo/endonuclease domain of bacterial DNA polymerase I and colocalizes with the kinetoplast topoisomerase II and DNA polymerase  $\beta$  during replication. *Proc. Natl. Acad. Sci. USA.* 96:8455–8460.
- Englund, P.T. 1979. Free minicircles of kinetoplast DNA in *Crithidia fasciculata*. *J. Biol. Chem.* 254:4895–4900.
- Englund, P.T., S.L. Hajduk, J.C. Marini, and M.L. Plunkett. 1982. Replication of kinetoplast DNA. In *Mitochondrial Genes*. P. Slonimski, P. Borst, and G.



- Attardi, editors. Cold Spring Harbor Laboratory, Cold Spring Harbor, NY. 423–433.
- Estevez, A.M., and L. Simpson. 1999. Uridine insertion/deletion RNA editing in trypanosome mitochondria—a review. *Gene*. 240:247–260.
- Ferguson, M., A.F. Torri, D.C. Ward, and P.T. Englund. 1992. In situ hybridization to the *Crithidia fasciculata* kinetoplast reveals two antipodal sites involved in kinetoplast DNA replication. *Cell*. 70:621–629.
- Ferguson, M.L., A.F. Torri, D. Perez-Morga, D.C. Ward, and P.T. Englund. 1994. Kinetoplast DNA replication: mechanistic differences between *Trypanosoma brucei* and *Crithidia fasciculata*. *J. Cell Biol.* 126:631–639.
- Guilbride, D.L., and P.T. Englund. 1998. The replication mechanism of kinetoplast DNA networks in several trypanosomatid species. *J. Cell Sci.* 111:675–679.
- Gull, K. 1999. The cytoskeleton of trypanosomatid parasites. *Annu. Rev. Microbiol.* 53:629–655.
- Johnson, C.E., and P.T. Englund. 1998. Changes in organization of *Crithidia fasciculata* kinetoplast DNA replication proteins during the cell cycle. *J. Cell Biol.* 143:911–919.
- Johnson, C.E., and P.T. Englund. 1999. A refined localization of the mitochondrial DNA primase in *Crithidia fasciculata*. *Mol. Biochem. Parasitol.* 102: 205–208.
- Kable, M.L., S. Heidmann, and K.D. Stuart. 1997. RNA editing: getting U into RNA. *Trends Biochem. Sci.* 22:162–166.
- Kitchin, P.A., V.A. Klein, B.I. Fein, and P.T. Englund. 1984. Gapped minicircles. A novel replication intermediate of kinetoplast DNA. *J. Biol. Chem.* 259:15532–15539.
- Kitchin, P.A., V.A. Klein, and P.T. Englund. 1985. Intermediates in the replication of kinetoplast DNA minicircles. *J. Biol. Chem.* 260:3844–3851.
- Li, C., and P.T. Englund. 1997. A mitochondrial DNA primase from the trypanosomatid *Crithidia fasciculata*. *J. Biol. Chem.* 272:20787–20792.
- Melendy, T., C. Sheline, and D.S. Ray. 1988. Localization of a type II DNA topoisomerase to two sites at the periphery of the kinetoplast DNA of *Crithidia fasciculata*. *Cell*. 55:1083–1088.
- Pasion, S.G., G.W. Brown, L.M. Brown, and D.S. Ray. 1994. Periodic expression of nuclear and mitochondrial DNA replication genes during the trypanosomatid cell cycle. *J. Cell Sci.* 107:3515–3520.
- Pérez-Morga, D., and P.T. Englund. 1993a. The attachment of minicircles to kinetoplast DNA networks during replication. *Cell*. 74:703–711.
- Pérez-Morga, D., and P.T. Englund. 1993b. The structure of replicating kinetoplast DNA networks. *J. Cell Biol.* 123:1069–1079.
- Ploubidou, A., D.R. Robinson, R.C. Docherty, E.O. Ogbadoyi, and K. Gull. 1999. Evidence for novel cell cycle checkpoints in trypanosomes: kinetoplast segregation and cytokinesis in the absence of mitosis. *J. Cell Sci.* 112:4641–4650.
- Robinson, D.R., and K. Gull. 1991. Basal body movements as a mechanism for mitochondrial genome segregation in the trypanosome cell cycle. *Nature*. 352:731–733.
- Shapiro, T.A., and P.T. Englund. 1995. The structure and replication of kinetoplast DNA. *Annu. Rev. Microbiol.* 49:117–143.
- Shlomai, J. 1994. The assembly of kinetoplast DNA. *Parasitol. Today*. 10:341–346.
- Simpson, L., and P. Braly. 1970. Synchronization of *Leishmania tarentolae* by hydroxyurea. *J. Protozool.* 17:511–517.
- Steinert, M., and S. Van Assel. 1967. Coordinated replication of nuclear and mitochondrial desoxyribonucleic acids in *Crithidia luciliae*. *Arch. Int. Physiol. Biochim.* 75:370–371.
- Sugisaki, H., and D.S. Ray. 1987. DNA sequence of *Crithidia fasciculata* kinetoplast minicircles. *Mol. Biochem. Parasitol.* 23:253–263.
- Tzfati, Y., H. Abeliovich, D. Avrahami, and J. Shlomai. 1995. Universal minicircle sequence binding protein, a CCHC-type zinc finger protein that binds the universal minicircle sequence of trypanosomatids. Purification and characterization. *J. Biol. Chem.* 270:21339–21345.
- Woodward, R., and K. Gull. 1990. Timing of nuclear and kinetoplast DNA replication and early morphological events in the cell cycle of *Trypanosoma brucei*. *J. Cell Sci.* 95:49–57.